Biosorption of Cr(VI) Ions onto Walnut Flowers: Application of Isotherm Models

Madjene, Farid [*+]
Unité de Développement des Equipements Solaires, UDES, Centre de Développement des Energies Renouvelables, CDER, Tipaza, ALGERIE

Danane, Fetta
Centre de Développement des Energies Renouvelables, CDER, Bouzaréah, Algiers, ALGERIE

Chergui, Ahmed
Laboratory of Electrochemistry-Corrosion, Metallurgy and Inorganic Chemistry, Faculty of Chemistry (USTHB), Algiers, ALGERIE

Trari, Mohamed
Laboratory of Storage and Valorization of Renewable Energies, Faculty of Chemistry (USTHB), Algiers, ALGERIE

ABSTRACT: *Biosorption of Cr(VI) ions onto Walnut Flowers (WF) is studied in a batch system in relation to the physical parameters. The efficiency approaches 100% with 5 g WF/L at pH~1.5 for a Cr(VI) concentration of 100 mg/L in less than 1 h. The experimental data are analyzed using two-parameter models (Langmuir, Freundlich, and Temkin), and three-parameter models (Redlich–Peterson, Sips, and Toth). In order to determine the best isotherm, two error analysis methods are used to evaluate the correlation coefficient and chi-square test. The error analysis demonstrates that the three-parameter models better describe the Cr(VI) biosorption data. The Sips equation provides the best fitting. The possible interaction between the Cr(VI) and the biosorbent surface was evaluated by FT-IR analyses. Overall, the proposed biosorbent material was successfully used for the removal of a Cr(VI) from contaminated solutions.*

KEYWORDS: *Biosorption; Cr(VI); Isotherm; Models; Walnut flower.*

INTRODUCTION

The industrial discharge of heavy metals into the aquatic medium is a worldwide pollution problem affecting dramatically the water quality. Many metals such as chromium, lead, cadmium, and mercury are highly toxic and can accumulate in humans and plants through ingestion of foods and drinking water causing serious damage to humans [1]. They cannot be biodegraded unlike organic molecules and the industrial effluents must be treated at the source. Chromium is reported to be highly toxic and is released in the aquatic environment from many

* *To whom correspondence should be addressed.*
+E-mail address: faridmadjene@yahoo.fr
1021-9986/2022/12/3963-3971 9/$/5.09

industries including electroplating, leather tanning, cement preservations, steel fabrication, etc. There exist various oxidation states for chromium in nature, among which Cr(III) and Cr(VI) [2]. The hexavalent state is highly mobile in soil and soluble in water, and is about 500 times more toxic than Cr(III) [3]. It is well established now that its toxicity provokes cancer as well as kidney, liver and gastric damages [4]. Hence the guidelines for water prescribed by the World Health Organization for Cr(VI) is limited at 0.05 mg/L [5]. Conventional methods for removing chromium including electroreduction, ion exchange, reverse osmosis and solvent extraction are either expensive or do not often reach the threshold set up by the water standards [6]. In this regard, biosorption is found to be an effective and inexpensive for Cr(VI) uptake. Many natural materials available in large quantities may have great potential as low cost biosorbents.

The exploitation of natural biomasses for the water treatment has gained growing importance for the environmental protection. Several studies are carried out using available biomaterials such as, Red peanut skin [7], Almond Shell [8], Spirulina platensis [9], leaves of Agave Americana L [10], Durian shell [11], Cuttlefish Bone Powder [12], Seaweed [13], chestnut shell [14], and walnut shell [14, 15]. Their attractive features are the high versatility, metal selectivity and large uptake efficiencies.

The present study deals with the biosorption of Cr(VI) from aqueous solution using batch process by inexpensive biosorbent developed from abundant biomass namely walnut flowers (WF). The experimental data are analyzed with two-parameter models (Langmuir, Freundlich and Temkin) and three-parameter models (Redlich–Peterson, Sips and Toth). Non-linear analysis is performed to obtain the equilibrium parameters and to find the appropriate model for the Cr(VI) uptake on WF.

EXPERIMENTAL SECTION

The walnut flower, obtained from local farms (Algiers), is thoroughly washed with water and dried at 80 °C overnight. Then it is crushed, ground in an agate mortar and sieved to select a particle size of 500 µm using ASTM standard sieve. The Cr(VI) stock solution (1 g/L) is prepared by dissolving K_2CrO_4 (Merck, 99 %) in water. Concentrations down to 50 mg/L are made up by dilution. The batch experiments are done in a beaker (250 mL capacity) under constant magnetic stirring (500 rpm) to investigate the optimal conditions of pH, biosorbent amount and Cr(VI) concentration. The effect of pH is investigated in the pH range (1.5-7) by equilibrating WF in 100 mL of Cr(VI) solution (100 mg/L). The pH is adjusted to the desired value by addition of H_2SO_4 or NaOH. The biosorbent dose ranges from 1 to 7 g/L. The aliquots are withdrawn at regular time intervals, the solutions are filtered and the supernatants analyzed for residual Cr(VI) concentration. Cr(VI) is determined by the diphenylcarbazide method [16], the violet color complex is titrated at 540 nm with a double beam spectrophotometer (Shimadzu 1800). The amount of Cr(VI) uptake and the percent biosorption are calculated from the Eqs. (1, 2):

$$q = (C_o - C)\frac{V}{m_s} \quad (1)$$

$$(\%) = \frac{C_o - C}{C_o} \times 100 \quad (2)$$

Fourier Transform InfraRed (FT-IR) spectra of WF before and after biosorption are recorded over the range 400–4000 cm^{-1} using a FT-IR spectrometer (JASCO-3400) and the KBr technique. All the solutions are prepared from reagents of analytical grade quality and distilled water.

All parameters are evaluated by the non-linear regression using Origine 7.5 Software. The optimization uses the error function to fit the experimental data. The correlation coefficients (R^2) and the chi-square test (χ^2) (Eq. 3) are used to measure the goodness-of-fit:

$$\chi^2 = \sum_{i=1}^{N} \frac{(q_e - q_i)^2}{q_i} \quad (3)$$

where: q_e is the observation from the batch experiment, q_i the estimate from the isotherm for corresponding q_e and N the number of observations in the experimental isotherm. If data from model are similar to the experimental ones, χ^2 will be small [17].

RESULTS AND DISCUSSION

Effect of contact time

The Cr(VI) biosorption by WF depends on the contact time and the results (Fig.1) show that the uptake rate increases rapidly in the early stage and then progressively until it reaches an equilibrium. The Cr(VI) removal occurs after 50 min of shaking. The high rate at the beginning is due to large WF surface area available after which the biosorption becomes

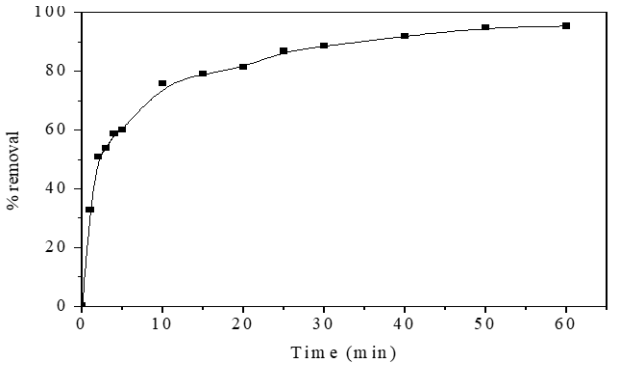

Fig. 1: Effect of contact time for biosorption of Cr(VI) onto WF ([Cr(VI)]= 100 mg/L, WF dose= 5 g/L, pH: 1.5 and 25 °C)

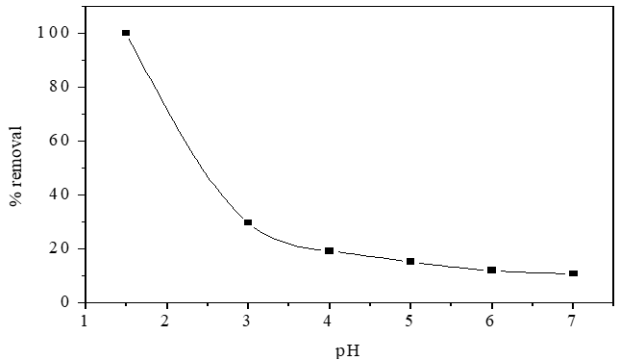

Fig. 2: Effect of pH for Cr(VI) biosorption onto WF under the following conditions: ([Cr(VI)]= 100 mg/L, WF dose= 5 g/L and 25 °C)

kinetically controlled by the rate of Cr(VI) transported to the internal sites of the biosorbent particles, thus requiring higher activation energies. Therefore, 1h is selected as the optimal time for further experiments.

Effect of pH on metal removal

The efficiency of chromium removal on WF for a concentration of 100 mg/L at different pHs is shown in Fig. 2. The biosorption declines from 100 to 10% as pH increases from 1.5 to 7. Such regression can be explained by the fact that at acidic pH, the WF surface is highly protonated, thus favoring an electrostatic interaction with the predominant anionic specie of Cr(VI), i.e. $HCrO_4^-$ [18]. This form is stable at low pHs according to the predominance diagram:

$$HCrO_4^- + H_2O \Leftrightarrow CrO_4^{2-} + H_3O^+ \qquad (pKa = 6.42)$$

This leads to high chromate uptake which decreases with increasing pH. Indeed, the OH^- concentration in the solution raises, thus increasing the dual competition of both anions ($HCrO_4^-$ and OH^-) to be adsorbed on the surface of WF. The above finding can also be supported by the point of zero charge (Determined from the standard technique [19] (pH_{pzc}= 6.90)) for WF that justifies the complete Cr(VI) removal at pH 1.5 i.e., the overall surface of WF is protonated, and consequently suitable to adsorb the $HCrO_4^-$ ions. By contrast, the WF surface charge becomes negatively charged with increasing pH and therefore, inhibiting drastically the biosorption by electrostatic repulsion. Similar results were obtained by *Luísa P. Cruz-Lopes et al.* using walnut or chestnut shells for Cr(VI) adsorption [14].

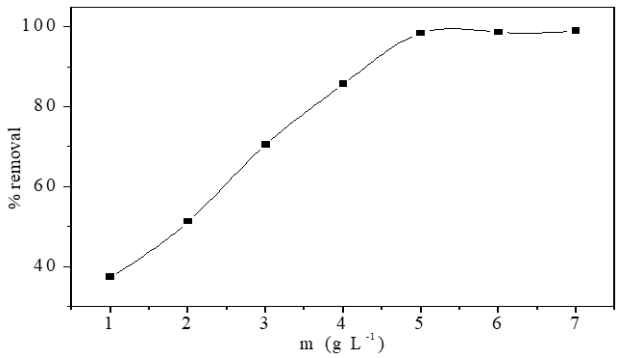

Fig. 3. Effect of biosorbent dose for Cr(VI) biosorption onto WF ([Cr(VI)]= 100 mg/L, pH: 1.5 and 25 °C)

Effect of biosorbent dose on metal removal

The effect of the biosorbent mass is illustrated in Fig. 3. With increasing the WF dose from 1 to 5 g/L, the percentage of Cr(VI) removal increases drastically from 37 to 100% because of the increasing number of binding sites and stabilizes above (5 g/L). Low uptake capacity at high biomass dose is attributed to the reduction of the overall surface area of the biosorbent by the aggregation during the biosorption, while the increase of removal efficiency is due to the increase of the vacant biosorption sites with more biomass existing in solution. So, the optimal biosorbent dose of WF is fixed at 5 g/L.

Effect of initial Cr(VI) concentration

The effect of Cr(VI) concentration (50–250 mg/L) is studied under optimized conditions i.e pH 1.5 with 5 g WF/L. The results (Fig.4) reveal that an increase of Cr(VI) concentration leads to a decrease in percentage of Cr(VI) removal from 83% to 57%, and raising in biosorption capacity from 9.16 to 28.41 mg/g.

The Cr(VI) diffusion into the WF pores would be accelerated by increasing initiale concentration, causing higher driving force would surpass the mass transfer resistance between WF surface and Cr(VI) ions [20]. In the other hand, this result can be due to the enhance Cr(VI) diffusion within the adsorbent pore sites under the

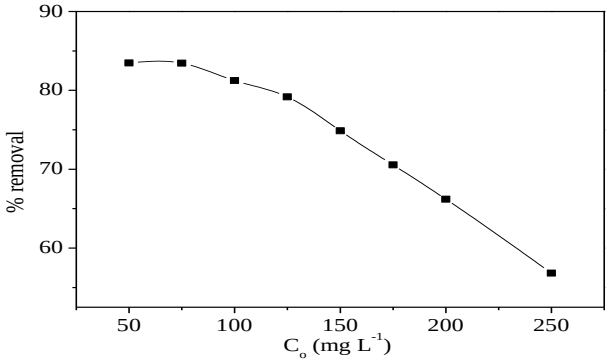

Fig. 4: Effect of Cr(VI) concentration for biosorption onto WF (WF dose= 5 g/L, pH: 1.5 and 25 °C).

influence of the concentration gradient of pollutant [21].

The regression in the activity is attributed to the rapid saturation of binding sites on WF. Above a threshold Cr(VI) concentration, all sites are occupied leading to a tendency toward saturation. By contrast, the increase of the biosorption capacity is due to the higher biosorption rate and the utilization of all active sites for biosorption at higher Cr(VI) concentrations.

Biosorption isotherms

Besides the well-known two-parameter models of Langmuir, Freundlich, and Temkin, three parameter models, namely Sips, Redlich–Peterson, and Toth are used to fit the experimental biosorption data. The linearization step of the isotherm equations leads to the alteration of the error distribution. Thus, to avoid such a problem, a non-linear regression analysis is performed for each model. In this study, the isotherm data are determined using the Origin 7.5 Software in order to optimize the non-linear iteration procedure.

Two-parameter models

a) The Langmuir model is based on a homogenous monolayer biosorption surface [22] (Eq. (4))

$$q_e = \frac{q_m \, \mathrm{b} \, \mathrm{C}_e}{1 + \mathrm{b} \, \mathrm{C}_e} \tag{4}$$

Fig. 5a illustrates the plots at 25 °C. The model fits relatively well the experimental data (Table 1), as high correlation coefficients and low chi-square values are obtained for the studied concentrations range, indicated the biosorption of Cr(VI) adopted a monolayer adsorption profile onto the homogeneous biosorbent surface and the affinity of all biosorption sites worms the Cr(VI) was

Table 1: Isotherm constants of two-parameter models for Cr(VI) biosorption onto WF (WF dose= 5 g/L, pH 1.5 and 25 °C)

Isotherm	Parameter	Values
Langmuir	q_m	34.635
	b	0.047
	R^2	0.995
	χ^2	0.103
Freundlich	n_f	2.693
	k_f	5.402
	R^2	0.930
	χ^2	1.343
Temkin	b_{Te}	0.331
	a_{Te}	0.421
	R^2	0.985
	χ^2	0.634

Table 2: The separation factor versus initial Ni^{2+} concentration (WF dose= 5 g/L, pH 1.5 and 25 °C)

C_o (mg/L)	50	75	100	125	150	175	200	250
R_L	0.137	0.096	0.074	0.060	0.050	0.043	0.038	0.099

equal [23]. The parameter *b*, representing the biosorption affinity of the binding sites, indicates a fair ability of WF biomass for the removal of Cr(VI).

The Langmuir model whose main feature can be expressed in terms of dimensionless separation constant (R_L) is given by (Eq. (5)) [24]:

$$R_L = \frac{1}{1 + \mathrm{b} \, \mathrm{C}_o} \tag{5}$$

The R_L value indicates the type of isotherm: unfavorable ($R_L > 1$), linear ($R_L = 1$), favorable ($0 < R_L < 1$) or irreversible ($R_L = 0$). The calculated R_L values for different Cr(VI) concentrations are shown in Table 2. It can be seen that R_L drops in the range 0–1 in all experiments, thus confirming the favorable uptake Cr(VI) by WF.

b) The Freundlich model is suitable for heterogeneous surfaces [25] (Eq. 6):

$$q_e = k_f \, \mathrm{C}_e^{1/n_f} \tag{6}$$

The values of $1/n_f$ and k_f correspond to the biosorption intensity and maximum biosorption capacity respectively. Fig. 5a shows the plots at 25 °C and the isotherm parameters for modeling the experimental results with the equation (6) are given in table 1. It is generally stated that the values of n_f in the range 2–10 represent good,

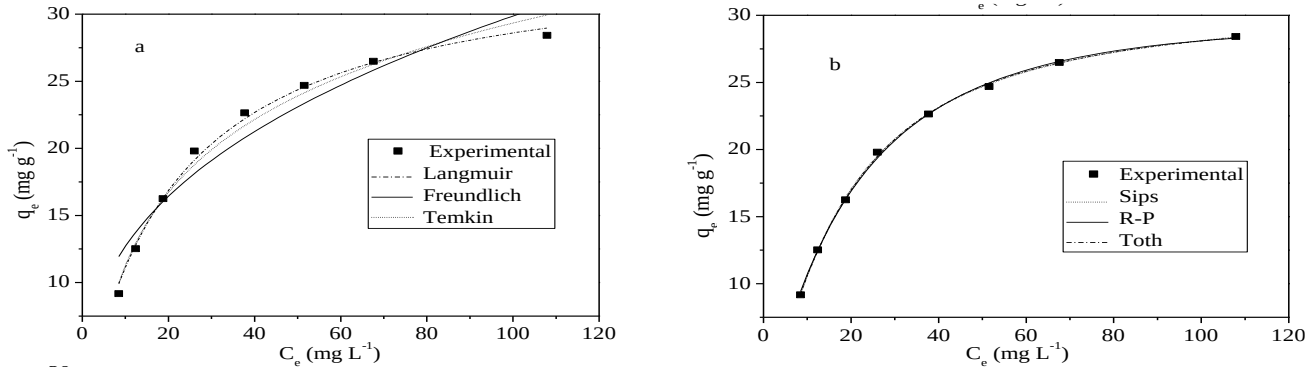

Fig. 5: Comparison of different models for Cr(VI) adsorption onto WF (WF dose= 5 g/L, pH 1.5 and 25 °C)

2-1 moderately difficult, and less than 1 poor biosorption characteristics [26]. The studied material is classified in the first category (good biosorbent) for Cr(VI) (n_f> 2). However, the correlation coefficients indicate that the data are badly correlated compared to the Langmuir model, suggesting the inapplicability of the Freundlich isotherm to describe the Cr(VI) biosorption on WF.

c) The Temkin isotherm [27] assumes that the decrease in the biosorption heat is linear rather than logarithmic, and supposes (i) the heat of biosorption in the layer decreases linearly with the coverage due to biosorbent–Cr(VI) interaction, (ii) the biosorption is characterized by a uniform distribution of binding energies, up to a maximum, this adsorption isotherm model only valid for intermediate concentration ranges. The isotherm is commonly applied in the following form (Eq. (7)):

$$q_e = \frac{\mathrm{RT}}{b_{\mathrm{Te}}} \ln (a_{\mathrm{Te}}\, \mathrm{C}_e) \tag{7}$$

The parameters are gathered in Table 1. The correlation coefficient (R^2) approaches 0.985, thus confirming the best fit of the equilibrium data, compared with the Freundlich one. However, the model remains less good than that of Langmuir. The variation of biosorption energy b_T is positive, indicating an exothermic biosorption reaction [28].

In the present investigation, the data are analyzed by two-parameter models namely the Langmuir, Freundlich and Temkin isotherms. The Langmuir model is the most appropriate to describe the isotherm data with high R^2 and low χ^2 values whose basic assumption is based on monolayer coverage of Cr(VI) onto the WF surface.

Three-parameter models

a) The Redlich–Peterson (R-P) model combines both the Langmuir and Freundlich ones and the hybrid mechanism does not follow a monolayer biosorption [29] (Eq. (8)):

$$q_e = \frac{K_R\, \mathrm{C}_e}{1 + a_R C_e^g} \tag{8}$$

It is helpful to outline that for g= 1, the equation converts simply to the Langmuir isotherm while for g= 0, it simplifies to the Henry's law. For $1 << a_R.\mathrm{C}_e^g$, it is identical to the Freundlich isotherm. The R–P equation provides a best fit over the whole concentrations range with R^2 close to unity (Fig. 5b and Table 3). g~ 1 and this means that the isotherm approaches rather the Langmuir model.

b) The Sips model converts to the Freundlich one at low concentrations and does not obey to the Henry's law. On the contrary, at high concentrations the model predicts a monolayer biosorption capacity, characteristic of the Langmuir isotherm [30] (Eq. (9)):

$$q_e = \frac{q_{\max}\, \mathrm{b}_s C_e^{n_s}}{1 + b_s C_e^{n_s}} \tag{9}$$

The maximum biosorption capacity (31.37 mg/g) is slightly smaller than that of Langmuir (34.63 mg/g). The n_s coefficient (1.23) indicates that the WF surface is homogeneous in nature and the Cr(VI) biosorption is more of Langmuir form rather than that of Freundlich. The main feature of the Sips isotherm is expressed by the dimensionless constant (R_S), referred to the equilibrium parameter or separation factor [31] (Eq. (10)):

$$R_S = \frac{1}{(1 + b_S\, \mathrm{C}_o)^{ns}} \tag{10}$$

The variation of R_S with C_o is shown in Table 4 R_S lies between 0.377 and 0.077 in the range (50-250 mg/L) and approaches zero with increasing C_o. The parameter R_S (< 1) indicates that WF is a suitable biosorbent for Cr(VI) species.

Table 3: Isotherm constants of the three-parameter models for Cr(VI) biosorption onto WF (WF dose= 5 g/L, pH 1.5 and 25 °C)

Isotherm	Parameter	Values
Redlich-Peterson	K_R	1.379
	a_R	0.021
	g	1.130
	R^2	0.999
	χ^2	0.046
Sips	q_{max}	31.374
	b_s	0.030
	n_s	1.232
	R^2	0.999
	χ^2	0.009
Toth	q_{max}	30.699
	b_T	0.041
	n_T	1.418
	R^2	0.999
	χ^2	0.010

Table 4: The separation factor versus initial Ni^{2+} concentration (WF dose= 5 g/L, pH 1.5 and 25 °C)

C_o (mg/L)	50	75	100	125	150	175	200	250
R_S	0.378	0.270	0.205	0.164	0.135	0.115	0.099	0.077

c) The Toth isotherm, derived from the potential theory, has yet to prove its success in describing the biosorption of metals in heterogeneous systems [32]. It assumes an asymmetrical quasi-Guaussian energy distribution with a widened left-hand side or in other words, a continuous distribution of the site affinity (Eq. (11)):

$$q_e = \frac{q_{\max}\ b_T C_e}{[1 + (b_T C_e)^{1/n_T}]^{n_T}} \qquad (11)$$

For n_T= 1, the isotherm converts to the Langmuir equation. The chi-square test (χ^2= 0.01) confirms the best equilibrium fit compared to the R-P model but is not as good as the Sips one as evidenced from χ^2 (Table 3). Indeed, the n_T value (1.418), indicates that the isotherm approaches the Langmuir one.

In the light of the data, all the three-parameter models gave appreciable fits with the experimental results. However, the best fit is obtained with the Sips model although the difference in the modeling with the other models is not very marked. The χ^2 values for the Toth and R-P models are greater than that of Sips.

Table 5: Biosorption capacities of different biosorbents for Cr(VI) removal from water

Biosorbent	q_{max} (mg/g)	References
tea factory waste	54.65	[33]
pistachio hull waste	116.30	[34]
coconut fibres	87.38	[35]
durian shell waste	10.75	[36]
Red Peanut Skin	117.00	[13]
Ocimum americanum L. seed pods	44.05	[7]
Aspergillus niger	83.33	[37]
Walnut shell	16.41	[38]
Walnut flowers	34.63	This study

Comparison of biosorption isotherms

The biosorption isotherms are fitted to two and three parameter models using Origin 7.5. The values of R^2 and χ^2 obtained from the isotherms show the best fits to the experimental values using the different equations and are satisfactory for Sips and Langmuir models. The fact that the Langmuir isotherm fits, well the experimental data may be due to the predominantly homogeneous distribution of active sites on the WF surface, since the model assumes a biosorbent surface energetically homogeneous.

The maximum Cr(VI) biosorption capacity (q_m) of WF is compared with other biosorbents reported in the literature (Table 5) where q_m has not been derived specifically. As one can see, the biosorption capacity of Cr(VI) on WF has an intermediate value. Furthermore, WF seems to be a performing biosorbent. In addition, the low cost, the local availability and renewability makes WF competitive with other biosorbents. Therefore, using this biomass to remove other pollutants is quite interesting for further studies.

Proposed mechanisms

FT-IR spectra are used to provide information on the biosorption mechanism on WF (Fig. 6). The strong band at 3420 cm^{-1} are due to N–H and O–H stretching vibrations of hydroxyl and amine groups on the biomass surface. Strong absorption bands at 2924.6 and 2854.4 cm^{-1} correspond to stretching of C-H bonds of the methyl and methylene groups. The weak peak centered at 2361.5 cm^{-1} is assigned to adsorbed CO_2 from air, confined in the pores of the samples [37]. Peaks at 1634 and 1590 cm^{-1} indicate the presence of C=O groups and N–H bending of amine groups respectively. The two peaks at 1457 and 1422 cm^{-1}

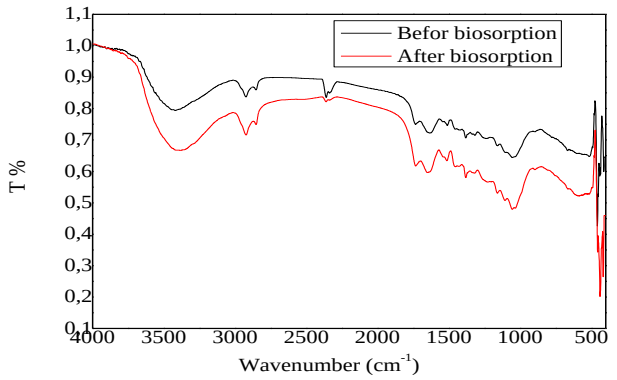

Fig. 6: FT-IR spectra of WF ([Cr(VI)]= 100 mg/L, WF dose= 5 g/L, pH 1.5 and 25 °C)

are attributed to the C–H deformation vibrations and COO groups respectively. A significant shift of these peaks from 1634 to 1651cm^{-1} and 1422 to 1430 cm^{-1} occurs probably due to the fact that carboxylic groups are protonated at pH 1.5 and make surface positively charged which is responsible for the biosorption of Cr(VI). The peak centered at 1382 cm^{-1} indicates the presence of C–H aliphatic bending whereas the peaks at 1318.6 and 1153 cm^{-1} are assigned to the C–N stretching vibration. The peaks at 1234 cm^{-1} representing C–O stretching, observed in aromatic rings due to –OCH_3 group also confirms the presence of lignin structure in WF which shifts to 1228 cm^{-1} in Cr(VI) loaded WF, indicating that these functional groups participate in Cr(VI) binding. The peak at 1055 cm^{-1} is assigned to the stretching vibration of C–OH of alcoholic groups. The disappearance of the peak at 516 cm^{-1} indicates C-N-C asymmetric stretching that is a consequence of Cr(VI)-loaded biomass. These amino groups are protonated at acidic pHs and the negatively charged chromate ($HCrO_4^-$) becomes electrostatically attracted by the positive charge amines in conformity with pH_{pzc}. The biosorption on WF may be due to complexation with functional groups. The relatively small shift in the wave number may be due to the perturbation of the bonding material energy when a ligand coordinates to a Cr(VI), the Cr(VI) ions was adsorbed on the WF surface by the functional groups that have shifted bands [39-41] and a physical biosorption could be expected. In the other hand, the differences in the band intensity can be attributed to interaction of Cr(VI) ions with functional groups on the adsorbent surface.

CONCLUSIONS

This study showed that an inexpensive and locally available agricultural by product namely walnut flower is successfully applied for Cr(VI) biosorption. The complete biosorption is obtained at pH 1.5 and the equilibrium is reached in less than 50 min. Moreover, the results indicated that, the equilibrium isotherm data are fitted using different models. The Langmuir and Sips models are the most appropriate to fit the experimental data. The FT-IR analysis confirmed the interactions between Cr(VI) and biosorbent surface. The results and the comparison to various biosorbents reported in the literature showed that the walnut flower biomass is an efficient biosorbent.

Nomenclature

The equilibrium binding constant (L/mg)	a_{Te}
The R–P constant (L/mg)	a_R
The Langmuir constant (L/mg)	b
The Sips constant	b_S
The Toth constant	b_T
The Temkin constant related to heat of biosorption (kJ/mol)	b_{Te}
Residual Cr(VI) concentration at equilibrium (mg/L)	C_e
Initial Cr(VI) concentration (mg/L)	C_o
The R–P exponent	g
The Freundlich constants $(\frac{L^{\frac{1}{n}}}{mg^{\frac{1}{n}-1}g})$	k_f
The R–P constant (L/g)	K_R
Biosorbent dosage (g/L)	m_s
The Freundlich constants	n_f
The Sips constant related to heterogeneity factor	n_S
The Toth exponent	n_T
Cr(VI) Amount adsorbed at equilibrium (mg/g)	q_e
The maximum biosorption capacity (mg/g)	q_m
Cr(VI) Amount adsorbed at any time (mg/g)	q_t
Universal gas constante	R
Correlation coefficient	R^2
Dimensionless separation factor of Langmuir	R_L
Dimensionless separation factor of Sips	R_S
Temperature (K)	T
Time of biosorption (min)	T
Volume of the solution (L)	V
The chi-square test	χ^2

Received: Sep. 22, 2021 ; Accepted: Jan. 10, 2022

References

[1] Ba S., Ennaciri K., Yaacoubi A., Alagui A., Bacaoui A., Activated Carbon from Olive Wastes as an Adsorbent for Chromium Ions Removal, *Iran. J. Chem. Chem. Eng. (IJCCE)*, **37(6):** 107-123 (2018).

[2] Esmaeili, A., Ghasemi, S., Zamani F., Investigation of Cr(VI) Adsorption by Dried Brown Algae Sargassum sp. and Its Activated Carbon. *Iran. J. Chem. Chem. Eng. (IJCCE)*, **31(4):** 11-19 (2012)

[3] Sarin V., Pant K.K., Removal of Chromium from Industrial Waste by Using Eucalyptus Bark, *Bioresource Technol. (BIRTEB)*, **97(1):** 15–20 (2006).

[4] Edebali S., Comparison of Chitosan-Based Biocomposites for Remediation of Water with Cr(VI) Ions, *Iran. J. Chem. Chem. Eng.*, **39(4):** 245-251 (2020).

[5] WHO, "Guidelines for Drinking-Water Quality", 4th Edition, Geneva, Switzerland (2011).

[6] Mohan D., Pittman Jr C. U., Activated Carbons and Low Cost Adsorbents for Remediation of Tri- and Hexavalent Chromium from Water, *J. Hazard. Mater. (JHMAD)*, **137(2):** 762–811 (2006).

[7] Kebir M., Chabani M., Nasrallah N., Bensmaili A., Trari M., Coupling Adsorption with Photocatalysis Process for the Cr(VI) Removal, *Desalination. (DSLNAH)*, **270(1-3):** 166–173 (2010).

[8] Ishaq M., Javed F., Amad I., Ullah H., Hadi F., Sultan S., Adsorption of Crystal Violet Dye from Aqueous Solutions onto Low-Cost Untreated and NaOH Treated Almond Shell, *Iran. J. Chem. Chem. Eng. (IJCCE)*, **35(2):** 97-106 (2016).

[9] Finocchio E., Lodi A., Solisio C., Converti A., Chromium (VI) Removal by Methylated Biomass of Spirulina Platensis: The Effect of Methylation Process, *Chem. Eng. J. (CMEJAJ)*, **156(2):** 264–269 (2010).

[10] Ben Nasr J., Ghorbal A., Adsorption of Indigo Carmine dye onto physicochemical-activated leaves of Agave Americana L, *Iran. J. Chem. Chem. Eng. (IJCCE)*, **40(4):** 1054-1066 (2020).

[11] Kurniawan A., Sisnandy V.O.A., Trilestari K., Sunarso J., Indraswati N., Ismadji S., Performance of Durian Shell Waste as High Capacity Biosorbent for Cr(VI) Removal from Synthetic Wastewatern, *Ecol. Eng.*, **37(6):** 940-947 (2011).

[12] Dehvari M., Ehrampoush M.H., Ghaneian M.T., Jamshidi B., Tabatabaee M., Adsorption Kinetics and Equilibrium Studies of Reactive Red 198 Dye by Cuttlefish Bone Powder, *Iran. J. Chem. Chem. Eng. (IJCCE)*, **36(2):** 143-151 (2017).

[13] Basha S., Murthy Z.V.P., Jha B., Biosorption of Hexavalent Chromium by Chemically Modified Seaweed, Cystoseira Indica, *Chem. Eng. J. (CMEJAJ)*, **137(3):** 480–488 (2008).

[14] Cruz-Lopes L.P., Macena M., Esteves B., Guiné R.P.F., Ideal pH for the Adsorption of Metal Ions Cr^{6+}, Ni^{2+}, Pb^{2+} in Aqueous Solution with Different Adsorbent Materials, *Open Agric. (OAJPCA)*, **6:** 115–123, (2021).

[15] Jahanban-Esfahlan A., Jahanban-Esfahlan R., Tabibiazar M., Roufegarinejad L., Amarowicz R. Recent Advances in the Use of Walnut (Juglans Regia L.) Shell as a Valuable Plant-based Bio-Sorbent for the Removal of Hazardous Materials, *RSC Adv. (RSCACL)*, **10:** 7026 (2020).

[16] Greenberg A. E., Clescerl L. S., Eaton A. N., "Standard Methods for the Examination of Water and Wastewater", 20th ed. American Public Health Association, New York. (1998).

[17] Ho Y.S., Chiu W.T., Wang C.C., Regression Analysis for the Sorption Isotherms of basic Dyes on Sugarcane Dust, *Bioresource Technol. (BIRTEB)*, **96(11):** 1285–1291 (2005).

[18] Rao P.S., Shashikant R., Munjunatha G.S., Kinetic studies on adsorption of chromium by coconut shell carbons from synthetic effluents, *J. Environ. Sci. Health A. (JESEDU)*, **27(8):** 2227–2241 (1992).

[19] Babić M.B., Milonjić S., Polovina M.J., Kaludierović B.V., Point of Zero Charge and Intrinsic Equilibrium Constants of Activated Carbon Cloth, *Carbon. (CRBNAH)*, **37(3):** 477–481 (1999).

[20] Jawad·A.H., Abdulhameed A.S., Wilson L.D., Hanafiah M.A.K.M., Nawawi W.I., ALOthman Z.A., Khan M.R., Fabrication of Schiff's Base Chitosan-Glutaraldehyde/Activated Charcoal Composite for Cationic Dye Removal: Optimization Using Response Surface Methodology, *J. Polym. Environ. (JPENFW)*, **29:** 2855–2868 (2021).

[21] Abdulhameed A.S., Hum N.N.M.F., Rangabhashiyam S., Jawad A.H., Wilson L.D., Yaseen Z.M., Al-Kahtani A.A., ALOthman Z.A. Statistical Modeling and Mechanistic Pathway for Methylene Blue Dye Removal by High Surface Area and Mesoporous Grass-based Activated Carbon using K_2CO_3 Activator, *J. Environ. Chem. Eng. (JECEBG)*, **9:** 105530 (2021)

[22] Shi Z., Zou P., Guo M., Yao S., Adsorption Equilibrium and Kinetics of Lead Ion onto Synthetic Ferrihydrites, *Iran. J. Chem. Chem. Eng. (IJCCE)*, **34**(3) : 25-31 (2015).

[23] Jawad A.H., Abdulhameed A.S., Hanafiah M.A.K.M., ALOthman Z.A., Khan M.R., Surip S.N. Numerical Desirability Function for Adsorption of Methylene Blue Dye by Sulfonated Pomegranate Peel Biochar: Modeling, Kinetic, Isotherm, Thermodynamic, and Mechanism Study, *Korean J. Chem. Eng. (KJCHE)*, **38(7):** 1499-1509 (2021).

[24] Ahmadi S.H., Davar P., Manbohi A., Adsorptive Removal of Reactive Orange 122 from Aqueous Solutions by Ionic Liquid Coated Fe_3O_4 Magnetic Nanoparticles as an Efficient Adsorbent, *Iran. J. Chem. Chem. Eng. (IJCCE)*, **35(1):** 63-73 (2016).

[25] Madjene F., Chergui A., Trari M., Biosorption of Ni(II) by Fig Male: Optimization and Modeling Using a Full Factorial Design, Water Environ. Res. (WAERED), **88(6):** 540-547 (2016)

[26] Yao Y., He B., Xu F., Chen X., Equilibrium and Kinetic Studies of Methyl Orange Adsorption on Multiwalled Carbon Nanotubes, *Chem. Eng. J. (CMEJAJ)*, **170(1):** 82–89 (2011).

[27] Matthews T., Majoni S., Nyoni B., Naidoo B., Chiririwa H., Adsorption of Lead and Copper by a Carbon Black and Sodium Bentonite Composite Material: Study on Adsorption Isotherms and Kinetics, *Iran. J. Chem. Chem. Eng. (IJCCE)*, **38(1):** 101-109 (2019).

[28] Kiran B., Kaushik A., Chromium Binding Capacity of Lyngbya Putealis Exopolysaccharides, *Biochem. Eng. J. (BEJOFV)*, **38(1):** 47–54 (2008).

[29] Chergui A., Madjene F., Trari M., Khouider A., Nickel Removal by Biosorption onto Medlar Male Flowers Coupled with Photocatalysis on the Spinel $ZnMn_2O_4$, *J. Environ. Health Sci. Eng. (JEHSBF)*, **12(13):** 1-10 (2014).

[30] Witek-Krowiak A., Szafran R.G., Modelski S., Biosorption of Heavy Metals from Aqueous Solutions onto Peanut Shell as a Low-Cost Biosorbent, *Desalination. (DSLNAH)*, **265(1-3):** 126–134 (2011).

[31] Zeng L., Li X., Liu J., Adsorptive Removal of Phosphate from Aqueous Solution using Iron Oxide Tailings, *Water Res. (WATRAG)*, **38(5):** 1318-26 (2004).

[32] Febrianto J., Kosasih A. N., Sunarso J., Ju Y. H., Indraswati N., Ismadji S., Equilibrium and Kinetic Studies in Adsorption of Heavy Metals using Biosorbent: A Summary of Recent Studies, *J. Hazard. Mater. (JHMAD)*, **162(2-3):** 616–645 (2009).

[33] Kumar R., Bishnoi N. R., Garima, Bishnoi K., Biosorption of Chromium(VI) from Aqueous Solution and Electroplating Wastewater using Fungal Biomass, *Chem. Eng. J. (CMEJAJ)*, **135(3):** 202–208 (2008).

[34] Javaid A., Bajwa R., Shafique U., Anwar J., Removal of Heavy Metals by Adsorption on Pleurotus Ostreatus, *Biomass and Bioenergy. (BMSBEO)*, **35**(5): 1675-1682 (2011).

[35] Costa A.W.M.C., Guerhardt F., Ribeiro Júnior S.E.R., Biosorption of Cr(VI) using Coconut Fibers from Agro-Industrial Waste Magnetized using Magnetite Nanoparticles, *Environ. Technol. (ENVTEV)*, **42(23):** 3595-3606 (2021).

[36] Zhang R., Wang B., Ma H., Studies on Chromium(VI) Adsorption on Sulfonated Lignite, *Desalination.* (DSLNAH), **255(1):** 61–66 (2010).

[37] Rahmana M. S., Islam M. R., Effects of pH on Isotherms Modeling for Cu(II) Ions Adsorption using Maple Wood Sawdust, *Chem. Eng. J. (CMEJAJ)*, **149(1-3):** 273–280 (2009).

[38] Solat S., Reza R., Soheila Y., Biosorption of Uranium(VI) from Aqueous Solution by Pretreated Aspergillus niger Using Sodium Hydroxide, *Iran. J. Chem. Chem. Eng. (IJCCE)*, **34(1):** 65-74 (2015).

[39] Baran M.F., Duz M.Z. Removal of Cadmium (II) in the Aqueous Solutions by Biosorption of Bacillus Licheniformis Isolated from Soil in the Area of Tigris River, *Intern. J. Environ. Anal. Chem. (IJEAA)*, **101(4):** 533-548 (2021).

[40] Baran M.F., Duz M.Z. Biosorption of Pb^{2+} from Aqueous Solutions by Bacillus Licheniformis Isolated from Tigris River with a Comparative Study, *Int. J. Latest Res Eng Manag. (IJLREM)*, **4(5):** 108-121 (2019).

[41] Baran M.F., Duz M.Z. Uzan S., Dolak İ., Celik K.S., Kilinc E., Removal of Hg(II) from Aqueous Solution by Bacillus subtilis ATCC 6051 (B1), *J Bioprocess Biotech. (JBBOGP)*, **8:** 329 (2018).